ELSEVIER

Polymer 41 (2000) 649–661

polymer

Light scattering characterization of tetramethyl polycarbonate blends with polystyrene and with styrene–pentabromobenzyl acrylate copolymers

G.D. Merfeld, D.R. Paul*

Department of Chemical Engineering and Texas Materials Institute, The University of Texas at Austin, Austin, TX 78712, USA

Received 29 September 1998; accepted 23 February 1999

Abstract

Time resolved light scattering is used to study the phase separation of tetramethyl polycarbonate (TMPC) blends with polystyrene (PS) and with styrene–pentabromobenzyl acrylate copolymers (S–PBBA). Addition of PBBA to the copolymer reduces the lower critical solution temperature with TMPC and slows the rate of phase separation. Both thermodynamic and structural contributions to phase separation are considered. TMPC/PS diffusion coefficients estimated using the linearized Cahn–Hilliard theory are compared with light scattering measurements reported previously and with calculated mutual diffusion coefficients extrapolated from tracer diffusion measurements. The effect of the jump depth into the two phase region on the late stage coarsening process is shown to correlate with the duration of the early stage process of spinodal decomposition.

Keywords: Phase separation; Spinodal decomposition; Time resolved light scattering

1. Introduction

How copolymer structure and composition affect miscibility behavior, phase separation kinetics, and morphology development is valuable knowledge when developing polymer blends. The last two issues are of particular importance in multiphase blends where, from among other factors, the rate of phase formation or dissolution plays a significant role in determining the microstructure of a blend and, hence, its properties. Modifying the chemical structure of a blend component through copolymerization may be an effective way to control morphology. The use of a copolymer could manifest such control in any combination of ways including through the structural mobility of the polymer chains or through the molecular interactions of polymer repeat units. Certainly, the role of thermodynamics at the interface is appreciated in terms of interfacial tension and interfacial thickness. The study of light scattering from polymer blends undergoing phase separation has proven useful for learning about the kinetics of blend phase separation and phase coarsening [1–4]. Studies have looked at the process of coalescence and at how incorporation of a compatibalizing agent can suppress phase separation, reduce particle size, and stabilize or improve phase dispersion [5–9].

In this study, phase separation and morphology development issues are explored in blends of tetramethyl polycarbonate (TMPC) with polystyrene (PS) and with styrene–pentabromobenzyl acrylate (S–PBBA) copolymers using light scattering. Blends of TMPC and PS have been studied by various methods including the analysis of phase behavior [10–15], light scattering [16], small angle neutron scattering [17,18], and forward recoil spectroscopy [19,20]. This system forms miscible blends in all proportions and has a well-established lower critical solution temperature (LCST) of approximately 240°C. We reported in a previous study that TMPC can tolerate a limited amount of PBBA in a copolymer with styrene (between 34 and 45 wt.%) before miscibility at 150°C is compromised [21]. Adding PBBA to the copolymer up to this limit, however, lowers the phase separation temperature. The limited miscibility and depression of the LCST phase boundary is attributed, at least in part, to the strongly endothermic interaction of PBBA with other repeat units. For tailoring the formulations of multiphase blends, the presence of highly unfavorable interactions may actually have desirable effects. PBBA has demonstrated value for its ability to impart flame retardancy [22,23]; additional utility may arise from its use in a copolymer blend.

* Corresponding author. Tel.: +1-512-471-5392; fax: +1-512-471-0542.
E-mail address: paul@che.utexas.edu (D.R. Paul)

0032-3861/00/$ - see front matter
PII: S0032-3861(99)00162-7

2. Light scattering theory

Several reviews of light scattering theory [24,25] and its application to polymer blends can be found in the literature. By subjecting the laws of mass transfer to the thermodynamic constraints of spinodal phase separation, Cahn and Hilliard [26,27] developed the following expression:

$$\frac{\partial \phi}{\partial t} = M\frac{\partial^2 g}{\partial \phi^2}\nabla^2\phi - 2MK\nabla^4\phi + \text{nonlinear terms}, \quad (1)$$

where ϕ is the volume fraction, g the free energy per unit volume, M the diffusional mobility, and K the gradient energy coefficient. The product of the mobility and the second derivative of free energy with respect to concentration in Eq. (1) can be defined as an apparent diffusion coefficient, D_{app}, alternatively referred to as an interdiffusion or an effective diffusion coefficient. If nonlinear terms are neglected, the spinodal decomposition equation can be solved in terms of a light scattering growth factor $R(q)$ and its associated wavevector q

$$R(q) = -M\frac{\partial^2 g}{\partial \phi^2}q^2 - 2Mkq^4 = -D_{app}q^2 - 2MKq^4. \quad (2)$$

The wavevector is related to the scattering angle θ as shown

$$q = \frac{4\pi n \sin(\theta/2)}{\lambda}, \quad (3)$$

where n is the refractive index of the polymer and λ the wave length of the light source. The solution to Eq. (1) predicts that light scattering will grow exponentially in time according to the relation:

$$I(q,t) = I(q,0)\exp[2R(q)t]. \quad (4)$$

Further, the Cahn–Hilliard theory predicts a time invariant maximum, q_m, in the scattering spectra during the early stages of spinodal decomposition which correlates with a characteristic dimension d of the phase separated morphology

$$d = \frac{\lambda}{2n\sin(\theta/2)} = \frac{2\pi}{q_m}. \quad (5)$$

The D_{app} in Eq. (2) can be measured as a function of temperature in a series of light scattering experiments and then extrapolated to zero to obtain an estimate for the spinodal phase boundary. For the extrapolation, the temperature dependence of D_{app} must be considered in terms of the mobility and the second derivative of free energy with respect to composition. To derive an expression for temperature dependence of the latter, it is instructive to begin with the Flory–Huggins theory of mixing polymers

$$\Delta g_{mix} = RT\left[\frac{\phi_A \ln \phi_A}{\tilde{V}_A} + \frac{\phi_B \ln \phi_B}{\tilde{V}_B}\right] + B(T)\phi_A\phi_B, \quad (6)$$

where $\tilde{V}$ is the molar volume and $B(T)$ the temperature dependent interaction energy density. If it is assumed that $B(T)$ is not dependent on the blend composition, the second derivative of the free energy of mixing with respect to the composition can be expressed as

$$\frac{\partial^2 g}{\partial \phi^2} = RT\left[\frac{1}{\phi_A\tilde{V}_A} + \frac{1}{\phi_B\tilde{V}_B}\right] - 2B(T). \quad (7)$$

In the two-phase region of the phase diagram, both the second derivative of free energy in Eq. (7) and the apparent diffusion coefficient are negative. At the spinodal,

$$\frac{\partial^2 g}{\partial \phi^2} = 0 = RT_s\left[\frac{1}{\phi_A\tilde{V}_A} + \frac{1}{\phi_B\tilde{V}_B}\right] - 2B(T_s), \quad (8)$$

where T_s is the spinodal temperature. Using Eq. (8), the bracketed terms can be expressed in terms of $B(T_s)$ and substituted into Eq. (7) to obtain

$$\frac{\partial^2 g}{\partial \phi^2} = 2T\left(\frac{B(T_s)}{T_s} - \frac{B(T)}{T}\right). \quad (9)$$

Assuming an interaction energy temperature dependence of the form $B(T) = B_H - TB_S$ where B_H and B_S denote enthalpic and entropic contributions, respectively, it can be shown

$$\frac{\partial^2 g}{\partial \phi^2} = 2B_H\frac{(T - T_s)}{T_s}. \quad (10)$$

Thus, the thermodynamic driving force is proportional to the depth of the temperature jump into the two phase region $(T - T_s)$ Using this approximation, D_{app} can be expressed as

$$D_{app} = 2MB_H\frac{(T - T_s)}{T_s}. \quad (11)$$

A similar line of development, expressed alternatively in terms of the Flory–Huggins interaction parameter χ with a temperature dependence of the form $\chi = a + b/T$, leads to the analogous result

$$D_{app} = \frac{2MRb}{\tilde{V}_{ref}}\frac{(T - T_s)}{T_s}, \quad (12)$$

where R is the universal gas constant and $\tilde{V}_{ref}$ is a reference molar volume of the mixture.

Scaling laws have been developed to treat phase coarsening during the intermediate and late stages of phase separation [28,29]. They predict that q_m and its associated intensity I_m will change exponentially in time as shown

$$q_m \propto t^{-\alpha}, \quad (13)$$

$$I_m \propto t^{\beta}, \quad (14)$$

where α and β are constants. For intermediate stage scattering, the theory predicts $\beta > 3\alpha$, while for the late stage $\beta = 3\alpha$ is expected. The morphology and the associated mechanism of coarsening are reflected in the value of α. Values of α ranging from 1/5 to 1 have been predicted by various models and simulations [4]. Experimentally, the value of α has been observed to change from 1/3 in the intermediate stage to 1 in

Table 1
Polymers used in this study

Polymer	Molecular weight information		T_g onset (°C) [a]	Source
	$\bar{M}_w$	$\bar{M}_n$		
TMPC	37,900	13,700	190	Bayer AG
PS100K	100,000	95,000	103	Pressure Chemical Co.
PS330K	330,000	100,000	105	Cosden Oil and Chemical Co.
S–PBBA10[b]	95,800	61,600	108	Synthesized
S–PBBA20[c]	113,400	67,800	110	Synthesized

[a] Measured by DSC at a scan rate of 20°C/min.
[b] Contains 19.8 wt.% PBBA.
[c] Contains 33.9 wt.% PBBA.

the late stage as a system crosses over from one coarsening mechanism to another [30–34].

3. Experimental

The materials used in this study are summarized in Table 1. Two grades of PS are included: a commercial, polydisperse version with a $\bar{M}_w = 330{,}000$ and a speciality, nearly monodisperse sample with $\bar{M}_w = 100{,}000$. Details on the synthesis and characterization of the S–PBBA copolymers were reported previously [21]. The numerical part of the copolymer acronym used in Table 1 corresponds to the weight percent PBBA added to the monomer feed for synthesis; the actual amount incorporated into the copolymers is 19.8 and 33.9 wt.% PBBA for S–PBBA10 and S–PBBA20, respectively.

Blends were prepared for light scattering experiments by solvent casting films from 15 wt.% solutions in dichloroethane onto glass slides. To control the rate of solvent evaporation, the samples were covered and allowed to dry overnight. Residual solvent was removed by slowly heating the samples under vacuum (over the course of several days to prevent bubble formation in the thick films) to a final temperature of 150°C where they were annealed for at least three days. The resulting samples were smooth, clear, and uniform. Film thickness, ranging from approximately 0.15 to 0.20 mm, was controlled by adjusting the concentration of the casting solution. The glass transition temperature of the polymers and their blends were measured in a Perkin–Elmer DSC-7 using a scan rate of 20°C/min. Visual cloud points were determined by heating the blends on a programmable Mettler hot stage using a nitrogen purge to prevent degradation.

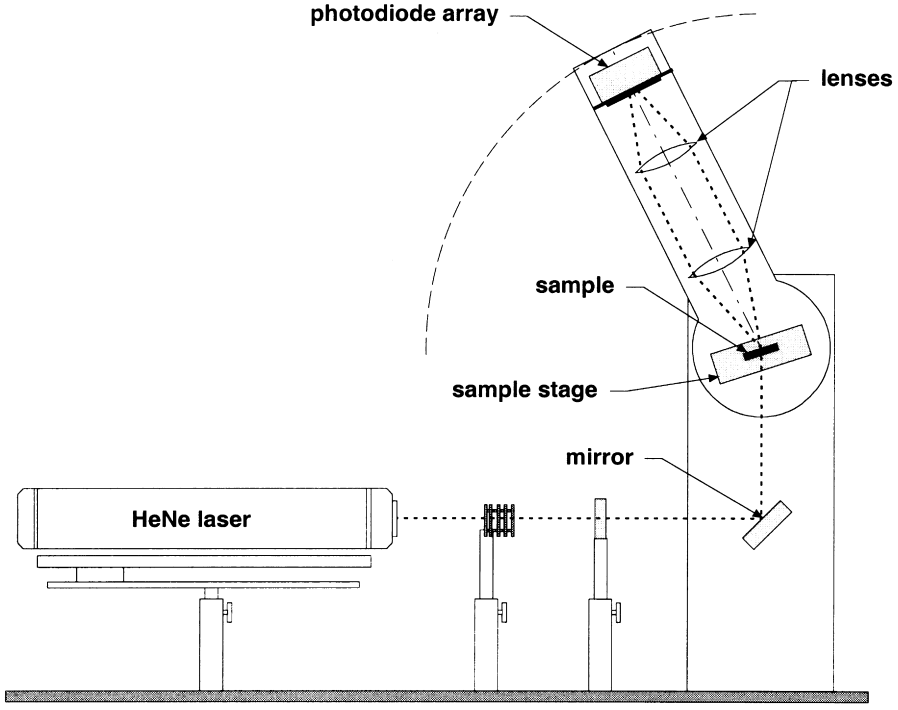

Fig. 1. Schematic of light scattering apparatus.

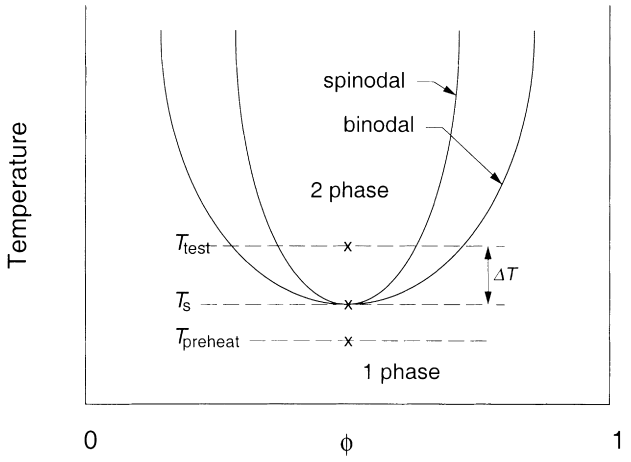

Fig. 2. LCST phase diagram illustrating temperature jump light scattering experiments.

Light scattering experiments were performed using equipment developed recently in our laboratory. The design, shown schematically in Fig. 1, is modeled after other systems reported in the literature [16,35,36]. The light source for the system is a 5 mW horizontally polarized HeNe laser which, after filtering, is reflected vertically through the polymer sample. The sample rests upon a stage which is modular in design to allow interchange between two heating stages: either a heated brass block that is well suited for isothermal or temperature jump experiments, or a programmable Mettler hot stage that may be used for controlled temperature ramp experiments. The entire sample stage assembly can be tilted with respect to the incident laser to enable the collection of wide angle scattering. A span of over 60° of scattering can be detected simultaneously using a system of large aperture lenses (Oriel Aspherab®, model 66063) and a linear diode array with 512 pixels (EG&G Park, model 1452A), all of which are mounted on an optical rail. The rail is attached to an indexing table whose axis is centered on the sample so that, when the detection system is swung to collect the desired range of scattering angles, the lenses remain properly focused on the sample.

Calibration of the diode array for scattering angle was performed using the interference pattern created by a diffraction grating while a correction for variation in pixel sensitivity, necessitated by the use of the lens system, was made using the uniform spectra from a chemi-phosphorecent liquid. The details of these methods are described elsewhere [37]. Control of the diode array and acquisition of scattering spectra was managed using EG&G Park OMA-Vision® software from Princeton Applied Research. After collecting a scattering spectrum, a data analysis program written in VISUAL BASIC programming language was used to smooth the intensity signal, correct for variation in pixel sensitivity, calibrate the scattering wavevector, and account for the refraction of the scattered light at the air/polymer interface. Algorithms in the program were also used to apply the Cahn–Hilliard and scaling law theories outlined in the preceding section.

Temperature jump light scattering experiments were performed as illustrated in the LCST diagram in Fig. 2. The blend was first preheated for 15 min at about 10°C below the phase separation temperature in a sample stage outside the light scattering apparatus and then quickly transferred to the test stage maintained at a higher temperature. Time-resolved light scattering was collected for a series of experiments using different sized temperature jumps.

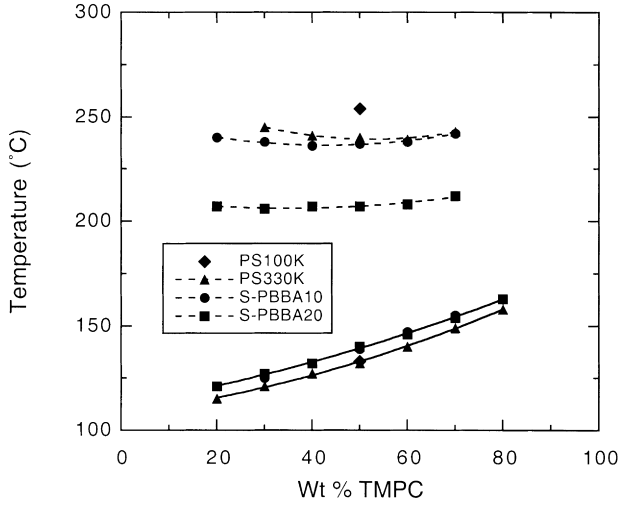

Fig. 3. Glass transition temperatures (connected by solid curves) and visually evaluated cloud points (connected by dashed curves) for blends of TMPC with the PS homopolymers and the S–PBBA copolymers listed in Table 1.

4. Results and discussion

4.1. Blend phase behavior

The glass transition and cloud point temperatures of blends of TMPC with PS100K, PS330K, and with both S–PBBA copolymers are summarized in Fig. 3. Because of limited material, only the 50/50 blend with PS100K was investigated. As expected, the glass transition temperature increases with the ratio of TMPC in the blend and with the addition of PBBA to the styrenic copolymer. Conversely, the cloud point is weakly dependent on blend composition and more strongly dependent on PS molecular weight and copolymer composition. Lowering the PS molecular weight from $\bar{M}_w = 330{,}000$ to $\bar{M}_w = 100{,}000$ shifts the LCST of a 50/50 blend upwards by nearly 15°C owing to the entropic contribution to the free energy. These results are in good agreement with previous reports on the TMPC/PS phase diagram [15,16] including the prediction of a binodal boundary that is relatively flat over the center range of blend compositions [20]. Using the TMPC/PS100K blend as a reference, since the PS100K molecular weight is comparable to that of the S–PBBA copolymers,

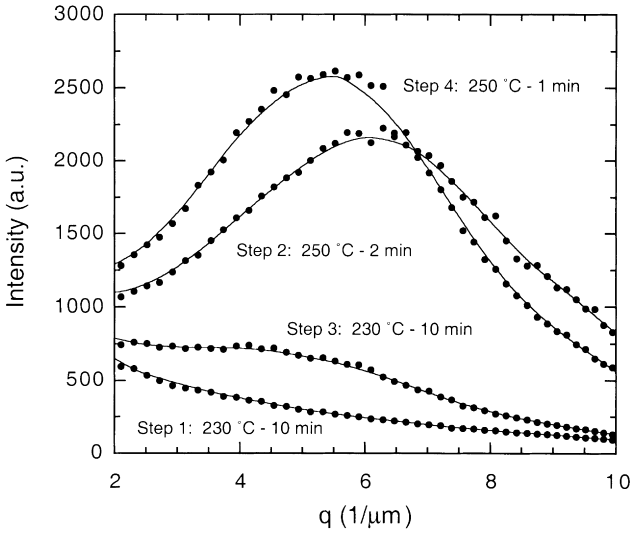

Fig. 4. Example of light scattering test for the reversibility of phase separation in a 50/50 blend of TMPC and S–PBBA10. In step 1, the blend is annealed at a temperature below the LCST, then in step 2 the temperature is jumped to above the phase boundary while phase separation is monitored by light scattering. The process is reversed by cooling in step 3. Finally, the jump into the two-phase region is repeated in step 4.

addition of 19.8 and 33.9 wt.% PBBA to the styrene copolymer (S–PBBA10 and S–PBBA20, respectively) lowers the phase separation temperature of blends with TMPC by approximately 15 and 45°C. Previously, we showed that equation-of-state calculations can be used to qualitatively predict this dependence [21].

Thermodynamic reversibility of phase separation was investigated by light scattering for all 50/50 blends. In these tests, the blend temperature was raised above the LCST phase boundary while watching for growth in the scattering intensity. Once light scattering indicative of the earliest stage of phase separation was observed, the blend was quenched to below the phase boundary and a gradual decay in the scattering spectrum observed as the blend rehomogenized. Heating the sample once again induced phase separation. An example of the process is summarized in Fig. 4 for a 50/50 blend of TMPC and S–PBBA10. In principle, the reversibility study could be repeated with smaller and smaller jumps above and below the phase boundary to accurately determine the phase separation temperature. Increasingly slow diffusion kinetics near the phase boundary, however, limited the practicality of this.

4.2. Early stage light scattering

To study the kinetics of spinodal decomposition, light scattering temperature jump experiments were performed on the blends with TMPC. Only 50/50 blend compositions were investigated to ensure optimal scattering efficiency. As changing PS molecular weight or the PBBA content in the copolymer has a considerable effect on the location of the LCST phase boundary, preheat and test temperatures were adjusted for each blend system. The conditions used in each experiment are summarized in Table 2. A preheat temperature well above the glass transition of the blend, more that 50°C above for TMPC/S–PBBA20 blends and closer to 100°C above for all other blends, helped to ensure that the kinetic measurements were not affected by the preheat conditions. For the relatively large temperature jumps used in this work, the linearized Cahn–Hilliard theory can be used without the correction for scattering due to thermal fluctuations offered by Cook [38,39]. It has been found experimentally that application of the Cahn–Hilliard–Cook modified theory is necessary only when the depth of the temperature jump into the two-phase region is small, less than about 0.5°C [3,32].

An example of the early stage scattering collected during a temperature jump experiment is shown in Fig. 5(a) for a blend of TMPC and PS330K. In this test, the sample was preheated at 230°C and then rapidly jumped to 250°C. During the first 200 s of phase separation shown, a time invariant maximum in the wavevector dimension and exponential growth of the scattering intensity are observed, both characteristic of early stage spinodal decomposition as predicted by the Cahn–Hilliard theory. The time evolution scattering profiles were evaluated according to Eq. (4) to estimate values of $R(q)$, and plots of $R(q)/q^2$ versus q^2 were constructed to evaluate D_{app} according to Eq. (2). Examples of the latter are shown in Fig. 6 for blends of TMPC with PS330K. To minimize random error, several samples were tested for each blend and the average value reported. Reproducibility was evaluated by running eight independent tests on a given blend. Standard deviations of approximately 10% in D_{app} and 2% in q_m were measured. The error found in D_{app} is not surprising considering the multiple regressions involved in its evaluation. In contrast, q_m is read directly as the maximum in the spectra and, therefore, it is not subject to the same analysis error. The apparent diffusion coefficients calculated for each blend are summarized in Table 2. Values of q_m are also reported along with the associated characteristic dimension d calculated using Eq. (5). For TMPC/PS blends, regardless of the molecular weight of the PS or the size of the temperature jump into the two phase region, characteristic dimensions between 1.0 and 1.1 μm were measured. Adding 19.8 and 33.9 wt.% PBBA to the styrene slightly reduced the characteristic dimension to 1.0 and 0.9 μm, respectively. This difference is real given the reproducibility of the measurements.

The D_{app} values reported in Table 2 are plotted versus temperature in Fig. 7(a). Over a broad temperature range, the D_{app} dependence is nonlinear in the TMPC/S–PBBA20 blends, but over a narrow temperature range of less than 15°C near the phase boundary all of the blends demonstrate a linear dependence such that the mobility contribution in Eq. (11) appears to be well approximated as a constant. Thus, a linear extrapolation of D_{app} to zero was used to estimate spinodal temperatures of 254, 241, 238, and 210°C for TMPC blends with PS100K, PS330K,

Table 2
Light scattering parameters

Blend	T_{test} (°C)	T_s (°C)	ΔT (°C)	$-D_{app}$ (cm^2 s^{-1})	q_m (μm^{-1})	d_m (μm)
TMPC/PS100K	255.0	254	1.0	5.8×10^{-13}	6.3	1.0
($T_{preheat}=240$°C)	257.5	254	3.5	2.2×10^{-12}	5.9	1.1
	260.0	254	6.0	4.0×10^{-12}	5.9	1.1
	262.5	254	8.5	5.5×10^{-12}	6.2	1.0
	265.0	254	11.0	7.3×10^{-12}	6.0	1.0
TMPC/PS330K	242.5	241	1.5	2.5×10^{-13}	6.4	1.0
($T_{preheat}=230$°C)	245.0	241	4.0	5.0×10^{-13}	6.2	1.0
	247.5	241	6.5	9.3×10^{-13}	6.4	1.0
	250.0	241	9.0	1.3×10^{-12}	5.9	1.1
	252.5	241	11.5	1.8×10^{-12}	5.9	1.1
	255.0	241	14.0	2.4×10^{-12}	6.2	1.0
TMPC/S–PBBA10	240.0	238	2.0	1.0×10^{-12}	6.1	1.0
($T_{preheat}=230$°C)	242.5	238	4.5	2.0×10^{-12}	6.2	1.0
	245.0	238	7.0	3.5×10^{-12}	6.3	1.0
	247.5	238	9.5	4.9×10^{-12}	6.4	1.0
	250.0	238	12.0	5.9×10^{-12}	6.0	1.0
TMPC/S–PBBA20	212.5	210	2.5	1.6×10^{-13}	7.2	0.9
($T_{preheat}=195$°C)	215.0	210	5.0	2.7×10^{-13}	7.2	0.9
	217.5	210	7.5	4.6×10^{-13}	7.1	0.9
	220.0	210	10.0	6.8×10^{-13}	7.2	0.9
	222.5	210	12.5	1.0×10^{-12}	7.2	0.9
	225.0	210	15.0	1.8×10^{-12}	7.1	0.9
	227.5	210	17.5	2.6×10^{-12}	7.0	0.9
	230.0	210	20.0	3.3×10^{-12}	7.0	0.9
	232.5	210	22.5	4.5×10^{-12}	7.0	0.9
	235.0	210	25.0	6.1×10^{-12}	6.9	0.9
	237.5	210	27.5	7.5×10^{-12}	6.9	0.9
	240.0	210	30.0	1.0×10^{-11}	7.0	0.9
	242.5	210	32.5	1.3×10^{-11}	6.7	0.9

S–PBBA10, and S–PBBA20, respectively. These estimates are in good agreement with the cloud point measurements shown in Fig. 3 and with previous reports in the literature for TMPC/PS blends [15,16].

Using the estimated spinodal temperatures, the data in Fig. 7(a), excluding the nonlinear range of the TMPC/S–PBBA measurements, are replotted in Fig. 7(b) versus $(T-T_s)$. The slope of these plots is proportional to the mobility as predicted by Eq. (11). This allows qualitative comparison of phase separation rates for a given temperature jump into the two phase region. Comparing TMPC blends with PS100K and S–PBBA10, a decrease in the mobility factor is observed when 19.8 wt.% PBBA is added to a copolymer with styrene. A more considerable decrease is noted in a comparison of TMPC blends with PS100K versus PS330K which arises largely from the increase in PS molecular weight by more than a factor of three. However, these changes are not entirely due to the obvious differences in the chain length or structure as some increase in the PS100K mobility is a result of the higher temperature range used in the light scattering experiments. The opposite is true for blends of TMPC with S–PBBA20 which were studied over a much lower range of temperatures than the other blends. By far, the TMPC/S–PBBA20 blends showed the slowest rate of phase separation. An increase in the blend glass transition temperature with the addition of more PBBA to the copolymer and the added steric hindrance associated with the brominated groups may contribute to this effect. To explore the structural difference between the PS100K and the S–PBBA copolymers, calculations of their fractional free volumes (FFV) can be compared. FFV is defined as $(V-V_o)/V$ where V is the experimentally measured specific volume and V_o is the occupied volume. Experimental measurements of density as a function of temperature at one atmosphere were used in a empirical relationship developed by Sanchez and Cho [40] to obtain FFV estimates of 0.219 for PS and 0.091 for a homopolymer of PBBA at 240°C. A similar difference was predicted using the group contribution method of Bondi [41]. Therefore, as styrene is copolymerized with increasing amounts of PBBA, diffusional mobility is expected to become more hindered owing to an increase in the glass transition temperature and a decrease in FFV.

When the temperature dependence of the blend interaction energies is known, the thermodynamic contribution to the diffusion coefficient can be estimated using Eq. (9) and compared for the different blend systems. If it is assumed that the temperature dependence of the interaction parameter arises from changes in the distance between molecules and not their spatial orientation, an equation-of-state

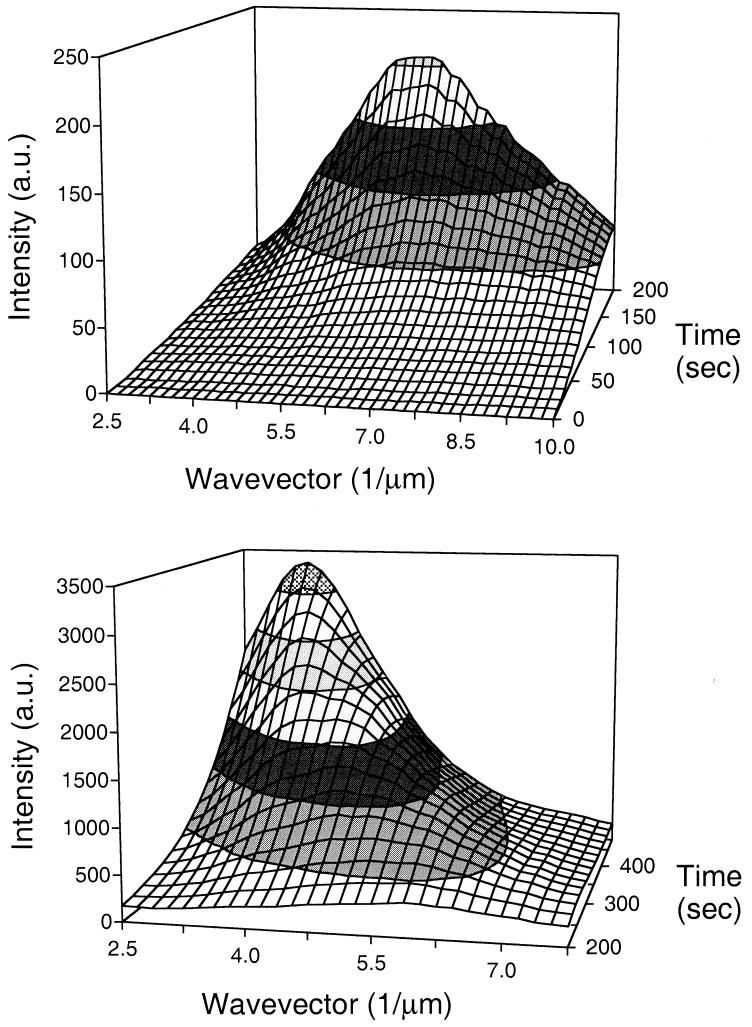

Fig. 5. Typical early (a) and intermediate and late (b) stage light scattering spectra collected from a 50/50 TMPC/PS330K blend in a temperature jump experiment.

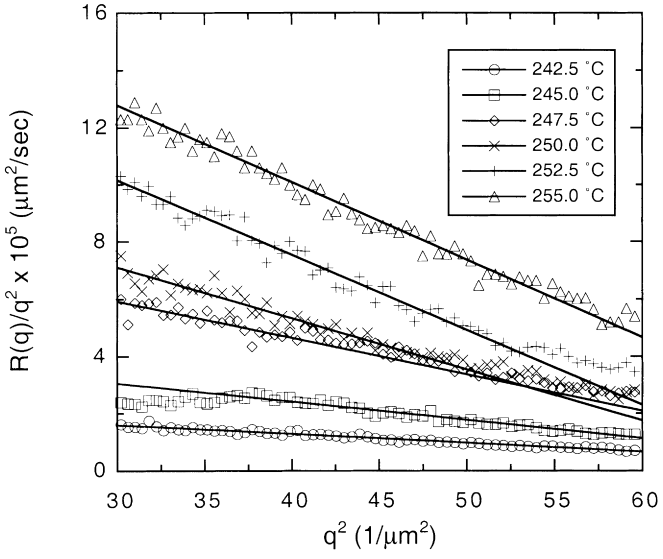

Fig. 6. Example of the Cahn–Hilliard analysis performed for blends of TMPC/PS330K for several different temperature jumps experiments. Apparent diffusion coefficients were evaluated for each experiment according to Eq. (2).

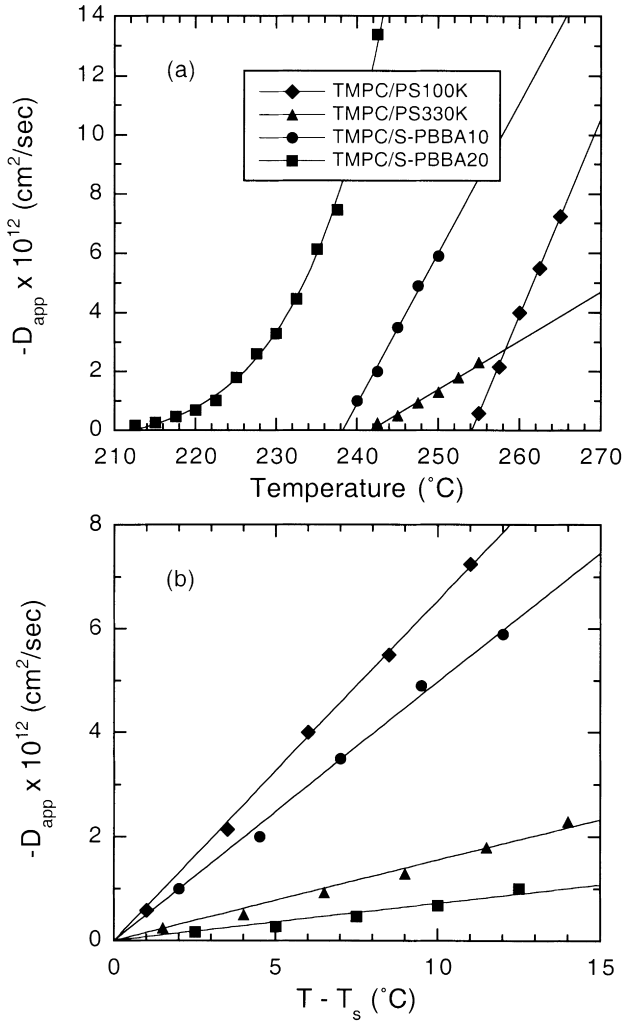

Fig. 7. Light scattering measured apparent diffusion coefficients plotted as a function of temperature (a), and as a function of the temperature above the spinodal temperature (b). Over a range of temperatures less than 15°C above the spinodal, the dependence is linear to a good approximation and, therefore, according to Eq. (11) the slope of a given plot is proportional to the molecular mobility.

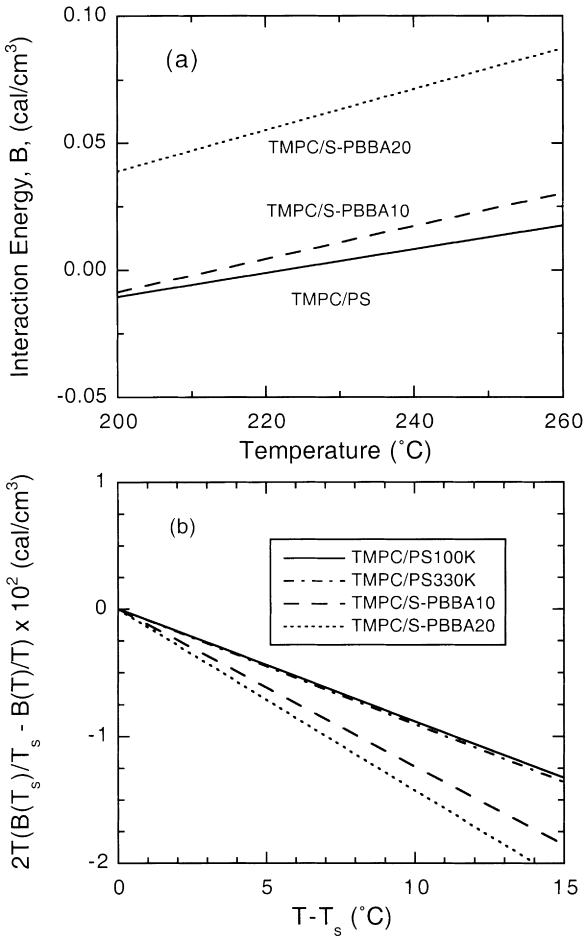

Fig. 8. (a) Equation-of-state prediction of the binary interaction energy for the blends investigated in this work as a function of temperature. (b) Calculation of the thermodynamic contribution to the diffusion coefficient given by Eq. (9) using the binary interaction energies summarized in (a). For comparison purposes, the thermodynamic contributions are plotted as a function of the temperature above the spinodal phase boundary.

can be used to estimate interactions as a function of temperature. The lattice fluid theory of Sanchez and Lacombe [42–44] was used for this work. The procedure involves calculating an interaction energy which, ideally, is independent of composition and temperature, to which equation-of-state effects are added in order to estimate the Flory–Huggins interaction energy at various temperatures. The details of these calculations have been given elsewhere [45,46]. The Sanchez–Lacombe characteristic parameters for TMPC, PS, and PBBA used in these calculations are compiled from previous reports [15,21,47,48] in Table 3 along with parameters for the S–PBBA copolymers

Table 3
Sanchez–Lacombe characteristic parameters

Repeat unit type	P (MPa)	T (K)	ρ (g/cm^3)	Temperature range (°C)	Reference
TMPC	440	729	1.185	220–270	[15]
PS[a]	379	795	1.097	200–250	[47,48]
PBBA	516	940	2.610	200–270	[21]
S–PBBA10[b]	391	809	1.239	200–250	–
S–PBBA20[b]	402	821	1.365	200–250	–

[a] Recalculated from data in reference.
[b] Calculated using PS and PBBA parameters and combining rules.

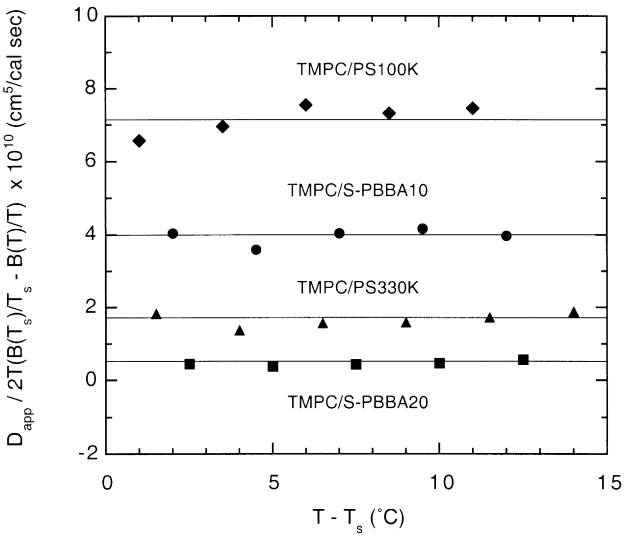

Fig. 9. Graphical comparison of the measured diffusion coefficient temperature dependence shown in Fig. 7(b) and that calculated using the equation-of-state predictions shown in Fig. 8(b). Over the range of less than 15°C above the LSCT, the temperature dependencies effectively cancel.

estimated using recommended combining rules. The binary interaction energies for each of the repeat unit pairs estimated from previous work [21] are: at 180°C $B_{TMPC/S} = -0.02$, and at 150°C $B_{TMPC/PBBA} = 3.4$ and $B_{S/PBBA} = 4.0$ cal/cm$_3$. Using a binary interaction model, the overall blend interactions were calculated as a function of temperature with the results shown in Fig. 8(a). These predictions can change slightly depending on the characteristic parameters used in the equation-of-state calculations. It is evident that incorporating PBBA into a copolymer with styrene makes the overall interaction with TMPC more endothermic but only slightly changes the temperature dependence. Based on these interaction energies, the quantity $2T(B(T_s)/T_s - B(T)/T)$ was calculated for each blend system and is plotted in Fig. 8(b) as a function of the temperature above the spinodal phase boundary. These results can be used to compare the relative role that molecular interactions play in the process of spinodal phase separation. The thermodynamic contributions are the highest for the TMPC blend with S–PBBA20 followed in decreasing order by S–PBBA10, PS330K, and PS100K, with the difference in the two polystyrenes being small. This order does not track with the actual diffusion coefficient measurements plotted in Fig. 7(b). This suggests that molecular mobility is more important than thermodynamics in determining the relative rates of spinodal decomposition in these blends.

The observation that thermodynamics is not the predominant factor in determining the relative rates of diffusion does not imply that these issues are insignificant in an absolute sense. In fact, as the mobility factor appears to be constant over a 15°C range above the LCST as shown in Fig. 7(b), the temperature dependence of D_{app} over this range must arise from thermodynamics. This can be proven by dividing the measured values of D_{app} by the corresponding calculated values of $2T(B(T_s)/T_s - B(T)/T)$. Fig. 9 shows that to a reasonable approximation this division cancels out the temperature dependence, thus demonstrating that the thermodynamic temperature dependence measured by light scattering is effectively the same as that predicted using the Sanchez–Lacombe equation-of-state theory. In this plot, the ordinate value corresponds to the mobility in units of cm^5/cal s for each blend system and serves to quantify the trends discussed previously in terms of the slope of the plots in Fig. 7(b).

4.3. Comparison of TMPC/PS diffusion coefficients

The apparent diffusion coefficients evaluated in this work for TMPC and PS blends can be compared with other measurements made by light scattering and forward recoil spectrometry (FRES). Guo and Higgins [16] used light scattering to study the phase separation kinetics of a blend of TMPC and PS having weight average molecular weights of 52,600 and 289,000, respectively. For this blend they measured a cloud point of approximately 240°C, which agrees well with that found in this study for a blend of comparable molecular weights (i.e. TMPC/PS330K). However, their spinodal temperature of 233°C is significantly lower than our measurement of 241°C. The diffusion coefficients measured by Guo and Higgins are plotted in Fig. 10(a) along with the TMPC/PS values from this work. For presentation on a logarithmic scale, the absolute values of the negative diffusion coefficients are plotted. Although their coefficients are smaller by two orders of magnitude, all the measurements share a similar temperature dependence.

In their analysis, Guo and Higgins do not mention correcting for the refraction of the scattered light at the air/polymer interface. This correction, the details of which have been given elsewhere [37,49], can have a considerable effect of the results of the Cahn–Hilliard analysis. For instance, when the light scattering data collected in this study were analyzed without the correction, the estimated diffusion coefficients were lower by more than an order of magnitude. Further, this led to characteristic phase dimensions on the order of 0.5 mm, similar to those reported by Guo and Higgins, rather than values on the order of 1 μm as reported in Table 2. This procedural difference in the light scattering analyses could explain some of the discrepancies between the two reports.

Kim et al. studied the diffusion of deuterated TMPC and PS tracer molecules in protonated blends of TMPC and PS by FRES for various tracer and matrix molecular weights, blend ratios, and temperatures [19]. Using the tracer measurements, they went on to extrapolate mutual diffusion coefficients [20] into the two-phase region and reported a significant discrepancy between these estimates and the apparent diffusion coefficients measured by Guo and Higgins. Here, our results are added to the comparison. These calculations, outlined in detail by Kim et al. [20],

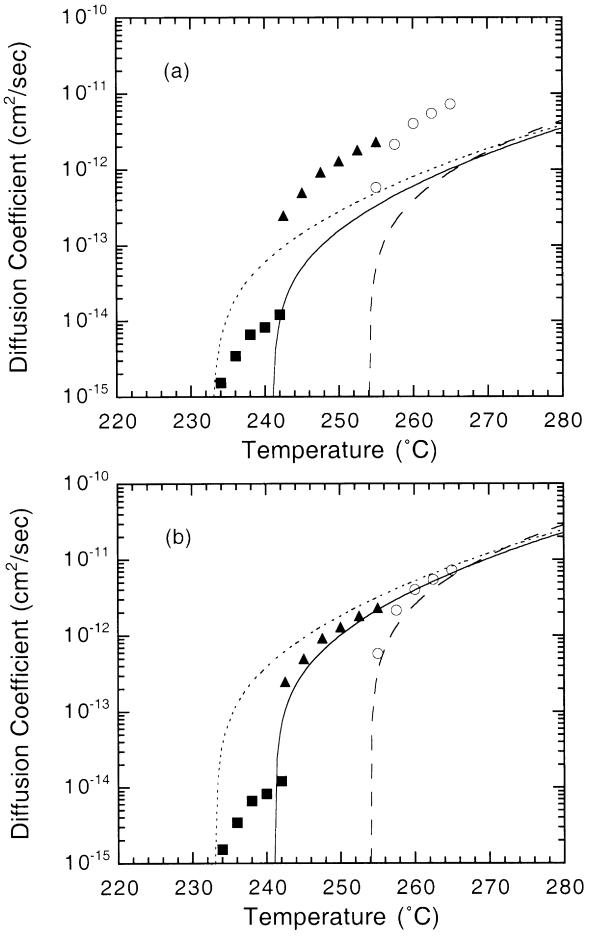

Fig. 10. Comparision of light scattering diffusion coefficients reported by Guo and Higgins in Ref. [16] (■) and those measured in this work for TMPC blends with PS100K (○) and PS330K (▲). For presentation purposes, the absolute values of the negative diffusion coefficients are plotted. FRES tracer diffusion measurements reported in Ref. [19] were used to estimate mutual diffusion coefficients for comparison to the light scattering measurements. The estimated curves correspond to the three sets of data: the dotted line is the calculated results for comparison with the solid squares (■), solid line with the solid triangles (▲), and dashed line with the open circles (○). Mutual diffusion coefficients were calculated using the interaction energy temperature dependence reported in this work (a), and using the much stronger temperature dependence reported in by Kim et al. in Ref. [20] (b).

require an estimate for the interaction energy temperature dependence to calculate the thermodynamic contribution to the diffusion coefficient, $\chi_s - \chi$. For this work, the TMPC/PS interaction energy density temperature dependence shown in Fig. 8(a) was used. To use the χ interaction nomenclature adopted in Kim's work, the B interaction energy density was converted to a χ using $\chi = B\tilde{V}_{ref}/RT$ with $\tilde{V}_{ref} = 168$ cm^3/mol. Tracer diffusion coefficients were estimated from monomer friction factors for a 50/50 blend and corrected to the molecular weights of each of the three TMPC/PS blend systems studied by light scattering. So that the calculated diffusion coefficients would properly go to zero at the phase boundary, the spinodal interaction energy χ_s was calculated for each blend system at the experimentally measured spinodal temperature. Calculations of the mutual diffusion coefficients are included in Fig. 10(a) for comparison with the three sets of light scattering measurements.

As Kim and coworkers noted, their calculated mutual diffusion coefficients are significantly larger than the light scattering measurements reported by Guo and Higgins. Similarly, the discrepancy is large between the calculated diffusion coefficients and the light scattering measurements reported in this study, but here the light scattering measurements are larger than the calculated values. In all cases, the calculated dependence on temperature and molecular weight compares favorably such that an arbitrary shift of the curves, either up or down as required, by roughly a factor of eight would align the curves with the light scattering measurements. A much stronger temperature dependence of the interaction energy than that used here, steeper than the slope in Fig. 8(a) by about a factor of 11, was estimated from the FRES measurements [20]. When this is applied to the calculations of the mutual diffusion coefficient, the predicted curves shift upward significantly as shown in Fig. 10(b), almost entirely correcting the disagreement with the diffusion coefficients measured in this study. However, a temperature dependence this large would require highly specific interactions that would be difficult to justify based on the chemical structures and the observed phase behavior. Alternatively, to correct the large discrepancy with the Guo and Higgins data, Kim et al. [20] investigated the potential effect of a spinodal phase separation process dominated by the growth of TMPC rich domains. This was found to significantly shift the mutual diffusion coefficients to smaller values. Certainly the opposite, a diffusion process dominated by PS rich domains, could be postulated to shift the calculations in the other direction. However, without employing empirical adjustments, the quantitative agreement is not favorable between the diffusion coefficients extrapolated from tracer diffusion coefficients and those measured by light scattering. More work is needed to elucidate the source of these discrepancies.

4.4. Intermediate and late stage light scattering

The light scattering spectra for the later stages of phase separation are characterized by a scattering maximum that shifts to smaller wavevectors. An example of such spectra is shown in Fig. 5(b) and can be contrasted with the early stage process shown in Fig. 5(a) for the same blend. As outlined earlier, the shift of the maximum and the growth of its intensity can be analyzed in terms of the scaling theories given by Eqs. (13) and (14). For blend systems that have similar phase separation temperatures, it was shown that experiments using equivalent jump depths can be used to make convenient comparisons of the phase separation rates [9]. For the blends studied here, the LCST can vary

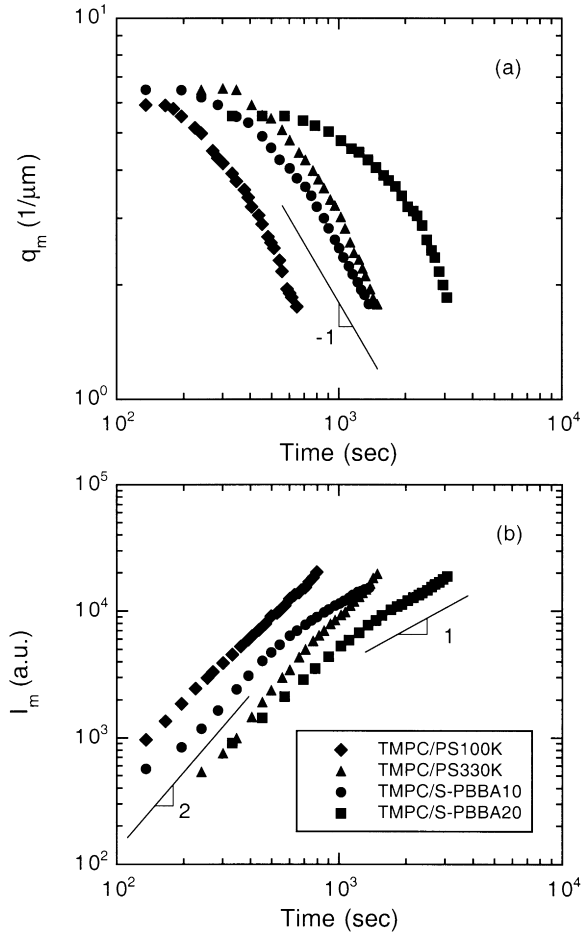

Fig. 11. Scaling law analysis of intermediate and late stage phase coarsening in TMPC blends with PS100K, PS330K and S–PBBA10 using temperature jumps of $\Delta T = 4°$ while for the blend of TMPC with S–PBBA20 using $\Delta T = 12$°C. The growth of q_m and I_m are analyzed according to the scaling law theories given by Eqs. (13) and (14).

significantly so this approach does not allow such a direct comparison but still provides a useful point of reference. Therefore, a constant temperature jump of 4°C above the LSCT was used to study TMPC blends with PS100K, PS330K and S–PBBA10 while, because of prohibitively slow rates of phase separation at lower temperatures, a larger jump of 12°C was used to study the TMPC/S–PBBA20 blend. Plots of q_m and I_m versus time are shown on double logarithmic scales in Fig. 11(a) and (b). Even with the larger temperature jump, the overall rate of phase separation is slowest for the blend with S–PBBA20 and increases for the other blends in the order PS330K, S–PBBA10, and PS100K. The same trend was observed in early stage spinodal decomposition. This is not surprising since the early stage process factors into the overall phase separation rate; however, it is possible for the early, intermediate, and late stages of phase separation to follow different kinetics.

When plotted in the terms of the scaling law given by Eq. (13), the q_m for the various blends share a similar time dependence as seen in Fig. 11(a). The transition from the early stage time invariant q_m to the late stage is continuous in all the blends such that a well defined intermediate regime is not evident. In the late stage, the slopes are fairly consistent with $\alpha = 1$. Likewise, I_m is plotted in Fig. 11(b) according its scaling law given by Eq. (14). During the first half of the coarsening process, a β of approximately two is noted for all of the blend systems. Over this same period, the corresponding value of α is less than 2/3 and so the theoretical prediction of $\beta > 3\alpha$ for the intermediate stage holds true. At later times, $\beta \sim 2$ persists in the TMPC blends with PS100K and PS330K but a deviation to $\beta = 1$ is observed in blends with the S–PBBA copolymers. The smaller β for the brominated blends indicates the amplitude of the composition fluctuations grows more slowly. Without knowledge of the physical morphology it is difficult to fully interpret this observation; however, it suggests that in addition to slowing the rate of early stage spinodal decomposition the presence of PBBA in the styrenic copolymer slows the late stage mechanism of coarsening from that of a blend with pure PS. The theoretical prediction that $\beta = 3\alpha$ in the late stage of phase coarsening is not satisfied by any of these blends.

To investigate the effect of the temperature jump depth on phase coarsening, blends of TMPC/S–PBBA10 were subjected to the same regimen of temperature jump experiments investigated in the early stage analysis. The conditions of these experiments were summarized previously in Table 2. Fig. 12(a) and (b) documents the scattering results in terms of a scaling law analysis. Each increase in the temperature jump by 2.5°C incrementally shifted both q_m and I_m curves to shorter times but did not noticeably change their shape. This is consistent with a faster rate of coarsening without a change in the mechanism of coarsening. A time constant, t_o, can be defined as the duration of the early stage spinodal decomposition process; this corresponds experimentally to the time when the wavevector maximum just began to shift with the onset of phase coarsening. It was found that normalizing each curve in Fig. 12(a) and (b) by its corresponding t_o caused the results for the various quench depths to more or less collapse onto a single curve as shown in Fig. 12(c) and (d). On the logarithmic time scale, this normalization is equivalent to subtracting log t_o from each curve. The collapsed data is significant because it demonstrates that the process of phase coarsening is linked to the early stage process of phase formation and, furthermore, that the duration of the early stage process can be used to scale the later stage processes. A characteristic time t_c can also be calculated as $t_c = 1/q_m^2 D_{app}$ using the parameters recorded in Table 2 from the Cahn–Hilliard analysis [50]. It has been predicted [51] that the early stage occurs for times up to approximately $2t_c$. However, calculated values of $2t_c$ were significantly different than experimentally measured t_o and did not produce the same collapse of the coarsening measurements.

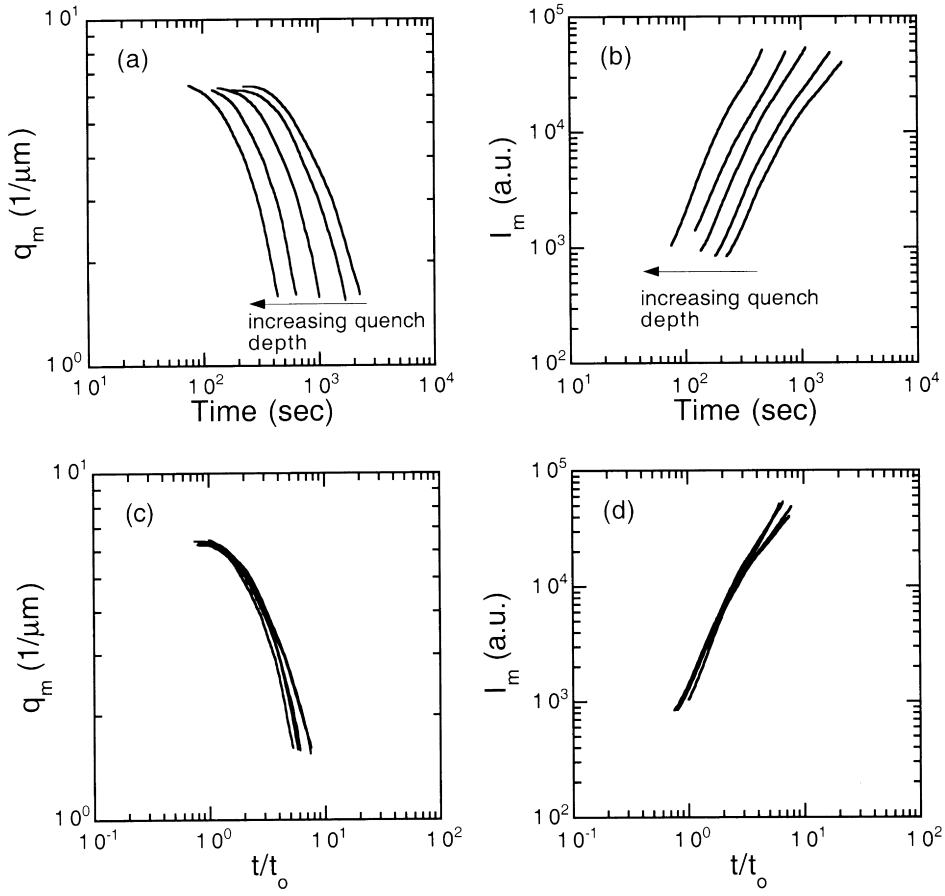

Fig. 12. The effect of the size of the temperature jump, ΔT, on the rate of phase separation in 50/50 blends of TMPC with S–PBBA20. Increasing ΔT from 2 to 12°C in 2.5°C increments shifts the q_m and I_m responses to lower times as shown in (a) and (b). Normalization of this data by the duration of the early stage spinodal phase separation process, t_o, can be used to collapse the data as shown in (c) and (d). The values of t_o measured for these experiments were 300, 225, 165, 120, and 75 s, correspondingly decreasing as the test temperature was increased from 240 to 250°C.

5. Conclusions

Time-resolved light scattering techniques were used to study the phase separation of blends of TMPC with PS and with S–PBBA copolymers. The relative rates of phase separation were compared as a function of the size of the temperature jump above the LCST phase boundary. Increasing PS molecular weight or adding PBBA into a copolymer with styrene was found to lower the LCST phase boundary of blends with TMPC and reduce the rate of spinodal phase separation. Additionally, the characteristic phase domain size of the blend was reduced as the content of PBBA in the copolymer was increased. Using an equation-of-state approximation to calculate the binary interaction energy temperature dependence, the thermodynamic portion of the diffusion coefficient was estimated and the temperature dependence of the measured diffusion coefficients was shown to arise from this thermodynamic contribution. The apparent diffusion coefficients measured in this work for TMPC/PS phase separation were significantly larger than light scattering measurements reported elsewhere and mutual diffusion coefficients estimated using FRES tracer diffusion measurements. The intermediate and late stages of phase separation were investigated using scaling law theories and, like the early stage process, an increase in PS molecular weight and addition of PBBA slowed the overall rate of phase coarsening; the effect was considerable for the S–PBBA copolymer containing 33.9 wt.% (8.7 mol%) PBBA. During the intermediate stage of phase coarsening, the mechanism of morphology development appears to be unaffected by the presence of the PBBA as evidenced by the slope of scaling law plots. But in the late stage, deviation to a slower growth mechanism indicated by a smaller exponential growth factor was observed in blends with the S–PBBA copolymers. For a given blend, increasing the depth of the temperature jump above the LCST expectedly increased the rate but did not change the scaling law analysis of the phase coarsening process. Further, the rate of the phase coarsening process was shown to scale with the duration of the early stage spinodal decomposition process.

Acknowledgements

The authors thank Dr C. Han and Dr L. Sung at the National Institute of Standards and Technology for their assistance in setting-up our light scattering apparatus. Financial support for this work was provided by the National Science Foundation grant numbers DMR 92-15926 and DMR 97-26484 administered by the Division of Materials Research—Polymers Program.

References

[1] Stein RS. Optical behavior of polymer blends. In: Paul DR, Newman S, editors. Polymer blends, New York: Academic Press, 1978.
[2] Hashimoto T. Dynamics in spinodal decomposition of polymer mixtures in phase transitions. Phase transitions, 12. UK: Gordon and Breach, 1988. p. 47.
[3] Hashimoto T. Structure of polymer blends. In: Cohn RW, Haasen P, Kramer EJ, editors. Materials science and technology, 12. New York: Weinheim, 1991 Chapter 6.
[4] Inoue T, Kyu T. Optical characterization: light scattering, birefringence and ellipsometry. In: Paul DR, Bucknall CB, editors. Polymer blends: formulation and performance, New York: Wiley, 1999 Chapter 11, to be published.
[5] Sondergaard K, Lyngaae-Jorgensen J. Influence of interface modification on coalescence in polymer blends. In: Nakatani AI, Dadmun MD, editors. Flow induced structure in polymers, Washington DC: ACS, 1995.
[6] Okamoto M, Inoue T. Polym Engng Sci 1993;33:175.
[7] Sung L, Han CC. J Polym Sci: Part B: Polym Phys 1995;33:2405.
[8] Macosko CW, Guegan P, Khandpur AK, Nakayama A, Marechal P, Inoue T. Macromolecules 1996;29:5590.
[9] Jackson CL, Sung L, Han CC. Polym Engng Sci 1997;37:1449.
[10] Casper R, Morbitzer L. Makromol Chem 1977;58/59:1.
[11] Humme G, Rohr H, Serini V. Makromol Chem 1977;58/59:85.
[12] Yee AF, Maxwell MA. J Macromol Sci Phys 1980;17:543.
[13] Wisniewsky C, Marin G, Monge P. Eur Polym J 1984;7:691.
[14] Fernandes AC, Barlow JW, Paul DR. Polymer 1986;27:1789.
[15] Kim CK, Paul DR. Polymer 1992;33:1630.
[16] Guo W, Higgins JS. Polymer 1990;31:699.
[17] Brereton MG, Fischer EW, Herkt-Maetzky C, Mortensen K. J Chem Phys 1987;87:6144.
[18] Yang H, O'Reilly JM. Mater Res Soc Symp Proc 1987;79:129.
[19] Kim E, Kramer EJ, Osby JO. Macromolecules 1995;28:1979.
[20] Kim E, Kramer EJ, Osby JO, Walsh DJ. J Polym Sci: Part B: Polym Phys 1995;33:467.
[21] Merfeld G, Maa TT, Chan K, Paul DR. Polymer, submitted for publication.
[22] Siegman A, Yanai S, Dagan A, Cohen Y, Rumack M, Georlette P. Poly(pentabromobenzyl acrylate), a novel flame-retardant additive for engineering thermoplastics. In: Price D, Iddon B, Wakefield BJ, editors. Int Conf, Chem appl. bromine and its compounds, Amsterdam: Elsevier, 1988. p. 339.
[23] Dave V, Israel SC, A CS. Polym Prepr 1990;31:554.
[24] van de Hulst HC. Light scattering by small particles. New York: Wiley, 1957.
[25] Tanford C. Physical chemistry of macromolecules. New York: Wiley, 1961.
[26] Cahn JW, Hilliard JE. J Chem Phys 1959;28:258.
[27] Cahn JW. J Chem Phys 1965;42:93.
[28] Binder K, Stauffer D. Phys Rev Lett 1974;33:1006.
[29] Langer JS, Bar-on M, Miller HS. Phys Rev A 1975;11:1417.
[30] Hashimoto T, Kumaki J, Kawai H. Macromolecules 1983;16:641.
[31] Okada M, Han CC. J Chem Phys 1985;85:5317.
[32] Kumaki J, Hashimoto T. Macromolecules 1986;19:763.
[33] Bates FS, Wiltzius P. J Chem Phys 1989;9:3258.
[34] Kyu T, Lim DS. Macromolecules 1991;24:3645.
[35] Snyder HL, Meakin P. Macromolecules 1983;16:757.
[36] Sato T, Han CC. J Chem Phys 1988;88:2057.
[37] Merfeld GD. PhD dissertation, The University of Texas at Austin, 1998.
[38] Cook HE. Acta Metall 1970;18:297.
[39] Binder K. J Chem Phys 1983;79:6387.
[40] Sanchez IC, Cho J. Polymer 1995;36:2929.
[41] Bondi A. Physical properties of molecular crystals, liquids and glasses. New York: Wiley, 1968.
[42] Sanchez IC, Lacombe RH. Macromolecules 1978;11:1145.
[43] Sanchez IC. Polymer phase separation. In: Meyers RA, editor. Encylopedia of physical science and technology, 13. New York: Academic Press, 1992.
[44] Sanchez IC, Panayiotou CG. Equation of state thermodynamics of polymer and related solutions. In: Sandler SI, editor. Models of thermodynamic and phase equilibrium calculations, New York: Marcel Dekker, 1994 Chapter 3.
[45] Callaghan TA. PhD dissertation, The University of Texas at Austin, 1992.
[46] Merfeld GD, Paul DR. Polymer 1998;39:1999.
[47] Gan PP, Paul DR. J Appl Polym Sci 1994;54:317.
[48] Gan PP. PhD dissertation, The University of Texas at Austin, 1994.
[49] Aoki O. PhD dissertation, The University of Massachusetts, 1990.
[50] Izumitani T, Hashimoto T. J Chem Phys 1985;83:3694.
[51] Hashimoto T, Tanaka H, Hasegawa H. In: Nagasawa M, editor. Molecular conformation and dynamics of macromolecules in condensed systems, New York: Elsevier, 1988. p. 257.